

Membrane tubule formation by banana-shaped proteins with or without intermediate network structure

Hiroshi Noguchi*

Institute for Solid State Physics, University of Tokyo, Kashiwa, Chiba 277-8581, Japan

The assembly of curved protein rods on fluid membranes is studied using meshless membrane simulations. Spontaneous curvature along the protein rod was focused in previous studies. Here, it is revealed that a small spontaneous curvature perpendicular to the rod can drastically alter the tubulation dynamics at high protein density whereas no significant difference is obtained at low density. A percolated network, which suppresses tubule protrusion, is intermediately formed depending on the perpendicular curvature. For a vesicle, a ring assembly stabilizing an outer bud is also obtained.

PACS numbers: 87.16.D-,87.15.kt,87.16.A-

In living cells, membrane shape deformations in endo/exocytosis, vesicular transport, cell motility, and cell division are regulated by various proteins [1–4]. Many of these proteins contain a binding module known as the BAR (Bin/Amphiphysin/Rvs) domain, which consists of a banana-shaped dimer [5–7]. The BAR domains are categorized into subset of unique families including “classical” BARs, F-BARs (Fes/CIP4 homology-BAR), and I-BARs (Inverse-BAR). The length of the BAR domains ranges from 13 to 27 nm [6]. The extension of membrane tubes from liposomes, formation of a cylindrical scaffold, and specific adsorption of the BAR superfamily proteins onto tube regions have been experimentally observed [5–11]. The dysfunction of the BAR proteins is considered to be implicated in neurodegenerative, cardiovascular, and neoplastic diseases. Thus, it is important to understand the mechanism of membrane shaping regulated by proteins not only for fundamental sciences but also for medical applications.

Frost et al. experimentally determined that F-BAR proteins adsorb more frequently on flat regions of lipid membranes than curved regions [8]. The protein assembly was observed on the flat membranes using electron microscopy. Although this assembly seems to be a nucleus of the tubule formation, the protrusion process of the tubules has not been experimentally observed. Recently, Tanaka-Takiguchi et al. reported that the formation dynamics of tubules from a liposome can be quite different for different F-BAR proteins [11]: FBP17 and CIP4 simultaneously generate many tubule protrusions over the entire surface, while PSTPIP1 and Pacsin2 generate only a few protrusions from a narrow region of the surface. Thus, the tubule nucleation process depends on the type of protein, although they belong to the same BAR family. However, it is not known what causes this difference of the tubule nucleation. They also reported that the full length of Pacin2 induces tubulation but its F-BAR domain region alone does not [11].

The BAR domains are banana-shaped and generate an anisotropic curvature different from the isotropic spontaneous curvature C_0 [12] induced by spherical colloids,

polymer-conjugated lipids, and other membrane-bending proteins. This anisotropic nature has recently received increasing theoretical interest. The classical Canham–Helfrich curvature free energy [13, 14] was extended to the anisotropic curvatures [15–17]. The adsorption and assembly of the BAR domains were investigated using atomic and coarse-grained molecular simulations [18–20]. Simunovic et al. simulated a linear aggregation of N-BAR domains parallel to the domains [20]. However, its relation with tubulation remains unsolved. Discoidal vesicles and tubular formation were simulated using a dynamically-triangulated membrane model [21, 22] and meshless membrane models [23, 24]. Despite these numerous advancements, the physics of membrane shape deformation caused by anisotropic curvature is still far from complete understanding.

In this Letter, we focus on the effects of the spontaneous (side) curvature C_{side} of the protein rod perpendicular to its longest axis. The excluded volume or van der Waals attraction between proteins can effectively generate positive or negative curvatures C_{side} . We demonstrate that even small values of C_{side} can qualitatively alter the tubulation dynamics, despite small changes in the thermal equilibrium properties. We simulate tensionless flat membranes, vesicles, and membrane tubes by using an implicit-solvent meshless membrane model [24–28]. A BAR domain is modeled as a banana-shaped rod, and it is assumed to be strongly adsorbed onto the membrane. In order to investigate the membrane-curvature-mediated interactions, no direct attractive interaction is considered between the rods. The membrane-mediated interactions induce the assembly of the protein rods [24].

We employ a spin meshless membrane model [24, 27], in which a membrane particle has an excluded volume with diameter σ and an orientational degree of freedom. Solvent is implicitly accounted for by an effective potential between the membrane particles. A fluid membrane is represented by a self-assembled one-layer sheet of N_{mb} particles. The bending rigidity κ and spontaneous curvature C_0 of the membrane are controlled by a curvature potential. A BAR protein is modeled as a

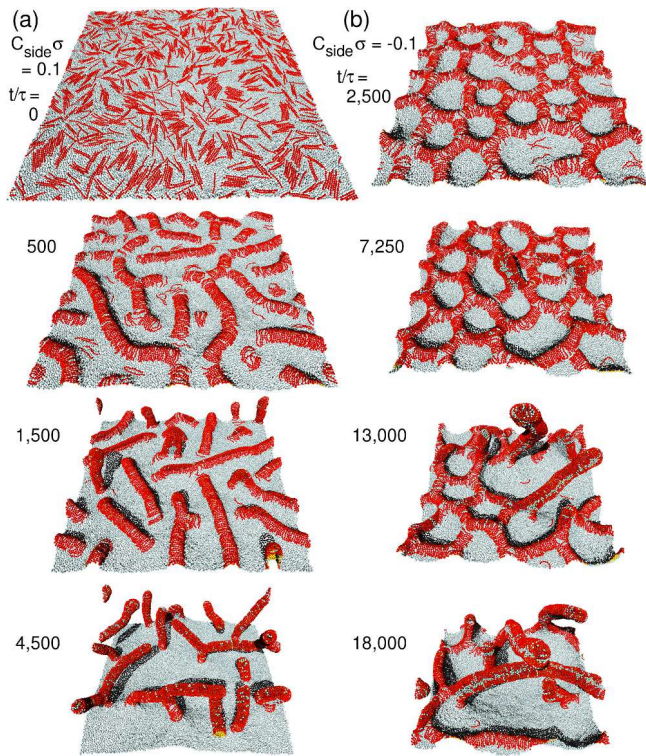


FIG. 1: (Color online) Sequential snapshots of tubulation from a tensionless flat membrane for (a) $C_{\text{side}}\sigma = 0.1$ and (b) $C_{\text{side}}\sigma = -0.1$ at $C_{\text{rod}}\sigma = 0.4$, $\phi_{\text{rod}} = 0.4$, and $N_{\text{rod}} = 1,024$. A protein rod is displayed as a chain of spheres, the halves of which are colored in dark gray (red) and in light gray (yellow). The orientation vector lies along the direction from the light (yellow) to dark gray (red) hemispheres. Light gray (light blue) particles represent membrane particles.

curved rod consisting of 10 membrane particles. The rod has anisotropic spontaneous curvature C_{rod} along the rod and C_{side} perpendicular to the rod. In this study, we employ the parameter set used in Ref. [24] for a membrane with $C_0 = 0$. The details of the model are given in Supplemental Material [29]. The membrane has mechanical properties that are typical for lipid membranes: the bending rigidity $\kappa/k_{\text{B}}T = 15 \pm 1$, the area of the tensionless membrane per particle $a_0/\sigma^2 = 1.2778 \pm 0.0002$, the area compression modulus $K_A\sigma^2/k_{\text{B}}T = 83.1 \pm 0.4$, and the edge line tension $\Gamma\sigma/k_{\text{B}}T = 5.73 \pm 0.04$, where $k_{\text{B}}T$ denotes the thermal energy. This edge tension is sufficiently large to prevent membrane rupture during tubulation. The molecular dynamics with a Langevin thermostat is employed [27, 30]. The simulation results are displayed with a time unit of $\tau = \sigma^2/D$, where D is the diffusion coefficient of the membrane particles in the tensionless membranes [29].

First, we investigated tubulation from a tensionless flat membrane at a high rod density, $\phi_{\text{rod}} = N_{\text{rod}}N_{\text{sg}}/N_{\text{mb}} = 0.4$, where the number of the rods $N_{\text{rod}} = 1,024$ and the number of the rod segments $N_{\text{sg}} = 10$ (see Figs. 1

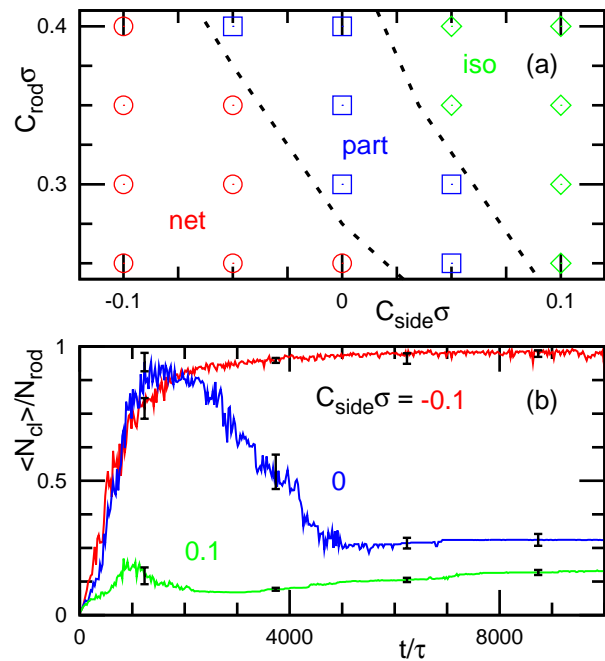


FIG. 2: (Color online) Dynamics of tubulation from tensionless flat membranes at $\phi_{\text{rod}} = 0.4$ and $N_{\text{rod}} = 1,024$. (a) Dynamic phase diagram. The (red) circles represent percolated network formation before the tubulation. The (green) diamonds indicate that tubules are formed from isolated clusters. The (blue) squares represent the partial network formation. The dashed lines are guides to the eye. (b) Time evolution of the mean cluster size $\langle N_{\text{cl}} \rangle$ for $C_{\text{side}}\sigma = -0.1$, 0, and 0.1 at $C_{\text{rod}}\sigma = 0.4$. Error bars calculated from eight independent runs are displayed at several data points.

and 2). The rods are equilibrated with $C_{\text{rod}} = 0$ and $C_{\text{side}} = 0$ initially, and the spontaneous curvatures are changed at $t = 0$. Immediately, the rods begin to assemble perpendicularly to the rod axis. For a positive spontaneous curvature of $C_{\text{side}}\sigma = 0.1$, many tubules simultaneously protrude via the bending of straight rod assemblies (see Fig. 1(a) and Movie S.1 [29]). Branches of the rod network are formed on the membrane only temporarily. When the tubulation is started, a neighboring branch is broken by its shrinking force. For a negative curvature $C_{\text{side}}\sigma = -0.1$, the rods form a percolated network covering the entire membrane area [see the top snapshot in Fig. 1(b)] and a tubule protrudes under membrane undulation (see the second snapshot in Fig. 1(b) and Movie S.2 [29]). Subsequently, the tubules grow along the network. Thus, the tubulation dynamics is remarkably changed by a relatively small side curvature C_{side} . Negative and positive side curvatures C_{side} stabilize and destabilize the network branches, respectively. The tubulation at $C_{\text{side}}\sigma = -0.1$ is much slower than that at $C_{\text{side}}\sigma = 0.1$ and much fewer tubules protrude: the average times of the protrusion of the first tubule are $\langle t_{\text{tb}} \rangle/\tau = 6,900 \pm 400$ and $1,000 \pm 100$ for $C_{\text{side}}\sigma = -0.1$

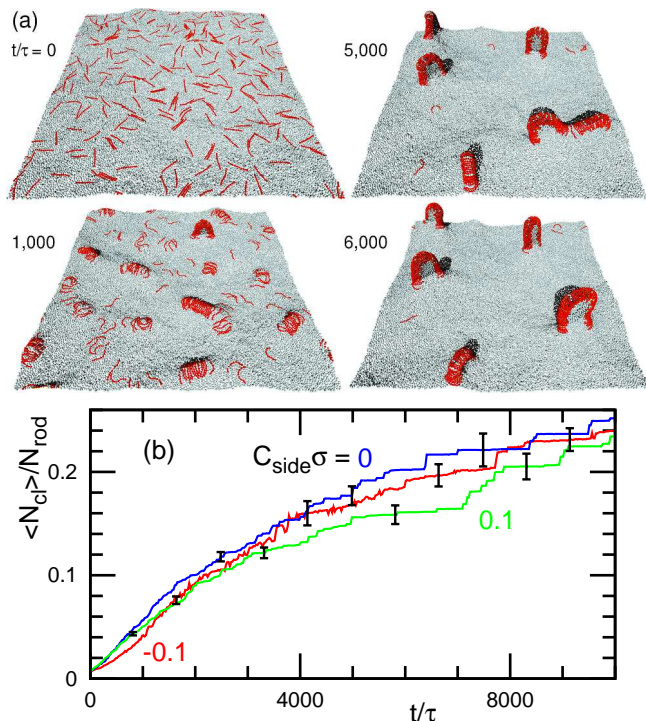


FIG. 3: (Color online) Membrane tubulation from a tensionless flat membrane for a low rod density, $\phi_{rod} = 0.1$, at $C_{rod}\sigma = 0.4$ and $N_{rod} = 256$. (a) Sequential snapshots at $C_{side}\sigma = 0$. (b) Time evolution of the mean cluster size $\langle N_{cl} \rangle$ at $C_{side}\sigma = -0.1, 0$, and 0.1 . Error bars calculated from eight independent runs are displayed at several data points.

and $C_{side}\sigma = 0.1$ at $C_{rod}\sigma = 0.4$, respectively.

Such characteristic dynamics is distinguishable from the time evolution of the mean cluster size $\langle N_{cl} \rangle$, as shown in Fig. 2(b). Two rods are considered to belong to the same cluster when the distance between the centers of mass of the rods is less than 5σ . For $C_{side}\sigma = -0.1$, most of the rods belong to one large percolated cluster during the tubulation. In contrast, for $C_{side}\sigma = 0.1$, $\langle N_{cl} \rangle$ decreases as the tubules are formed, and later $\langle N_{cl} \rangle$ slowly increases owing to tubule fusion into branched tubules [see the bottom snapshot in Fig. 1(a)]. Based on the evolution of $\langle N_{cl} \rangle$, the tubulation pathways are categorized to three groups [see Fig. 2(a)]: tubulation via percolated-network formation (net), via partial-percolated-network formation (part), and without percolation (iso). When a percolated network does not cover the entire membrane surface or a large cluster of $N_{cl} \simeq N_{rod}$ is maintained for a period shorter than $2,000\tau$, we categorize the tubulation pathway as the partial-percolated-network formation. As the rod curvature C_{rod} decreases, the tubulation becomes slower and a smaller number of large tubules are formed. The tubules are nucleated and grow from the branch of the network at $C_{rod}\sigma = 0.25$ or 0.3 and $C_{side}\sigma = -0.1$.

Our simulation results show that the network formation is crucial for the tubulation. To confirm this more

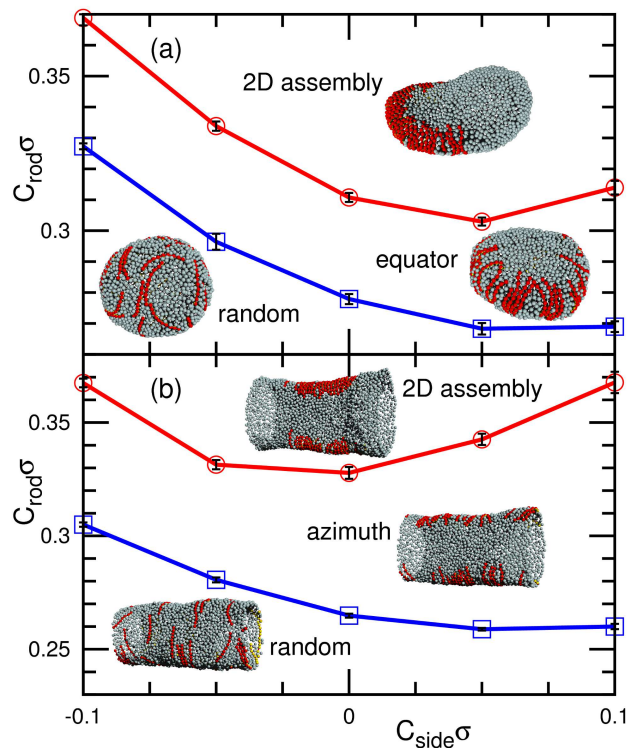


FIG. 4: (Color online) Phase diagram of (a) vesicles and (b) membrane tubes in thermal equilibrium at $\phi_{rod} = 0.167$ and $N_{rod} = 40$. The solid lines with squares and circles represent the boundary between the randomly mixed states and 1D assembly and the boundary between the 1D assembly and 2D assembly, respectively. Error bars are calculated from four independent runs. In the insets of (a) and (b), snapshots are shown for $C_{rod}\sigma = 0.2, 0.3$, and 0.4 at $C_{side}\sigma = 0$.

clearly, the effects of the side curvature C_{side} on the rod-membrane interaction are investigated. A percolated network is not formed during the tubulation at a low rod density, $\phi_{rod} = 0.1$. The rods assemble into linear clusters and subsequently large clusters ($N_{cl} \gtrsim 40$) transform into tubules (see Fig. 3(a) and Movie S.3 [29]). Although initial cluster formation is slightly slower for the negative curvature, $C_{side}\sigma = -0.1$, no qualitative difference is detected in the tubulation dynamics [see Fig. 3(b)].

Figure 4 shows the thermal equilibrium states on a vesicle of a radius $R_{ves} = 15.4\sigma$ and on a membrane tube of a radius $R_{cyl} = 9.89\sigma$ calculated using replica-exchange molecular dynamics [24, 31, 32]. At low values of C_{rod} , the rods are randomly distributed on a spherical vesicle and on a cylindrical tube. With increasing C_{rod} , an oblate vesicle or an elliptic tube is formed, and the rods assemble at largely bent membrane regions (the equator of the oblate or tips of the ellipse). Subsequently, they form a two-dimensional (2D) assembly. Thus, the assemblies are divided into two 1D assemblies unlike normal 2D phase separation [24]. The phase boundaries, which are determined by the inflection point and max-

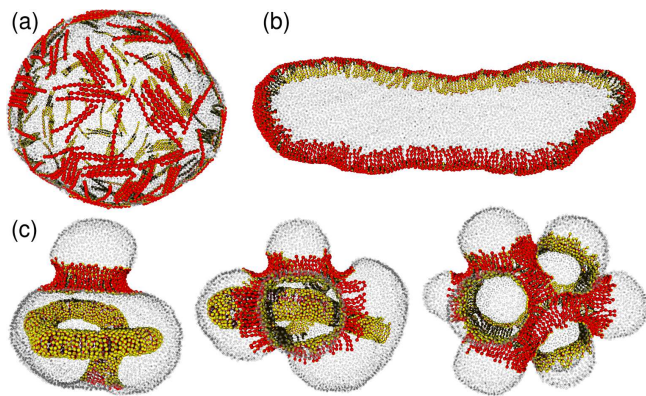


FIG. 5: (Color online) Snapshots of vesicles at $\phi_{\text{rod}} = 0.3$ and $N_{\text{rod}} = 288$. (a) Spherical shape in thermal equilibrium at $C_{\text{rod}} = 0$ and $C_{\text{side}} = 0$. (b) Elongated discoidal shape in thermal equilibrium at $C_{\text{rod}}\sigma = 0.4$ and $C_{\text{side}}\sigma = -0.1$. (c) Three metastable shapes at $C_{\text{rod}}\sigma = -0.4$ and $C_{\text{side}}\sigma = 0.1$. The membrane particles are displayed as small transparent spheres for clarity.

imum of the shape deformation [29], are only slightly dependent on the side curvature C_{side} ; therefore, the effects of C_{side} on the rod assembly are very limited. Thus, we conclude that the suppression of the tubulation at high rod density is caused not directly by the local rod-membrane interactions but by the mesoscale network formation.

Next, we investigated tubulation from a vesicle of radius $R_{\text{ves}} = 30.7\sigma$ at $\phi_{\text{rod}} = 0.3$ (see Fig. 5) and found that the original membrane curvature $C_{\text{ves}} = 1/R_{\text{ves}} = 0.033/\sigma$ changes the tubulation dynamics. For the positive curvature $C_{\text{rod}}\sigma = 0.4$, no tubulation is obtained for $C_{\text{side}}\sigma = -0.1, 0$, and 0.1 . Instead, the vesicle deforms into an elliptic disk, and the rods surround the rim of the disk [see Fig. 5(b)]. Similar shapes were previously reported by Monte Carlo simulations [22]. The rod network is temporally formed but is broken in a short period even for $C_{\text{side}}\sigma = -0.1$ (see Fig. S.3 in Supplemental Material [29]). Thus, the outward tubulation and network formation are suppressed in small vesicles.

In contrast, for the negative curvature $C_{\text{rod}}\sigma = -0.4$, tubulation into the inside of the vesicle is obtained (see Fig. 5(c) and Fig. S.4 in Supplemental Material [29]). A percolated network has a much longer lifetime than in the flat membrane [see the middle and right snapshots in Fig. 5(c)]. The coexistence of tubules and a ring is also obtained [see the left snapshot in Fig. 5(c)]. The ring stabilizes an outward bud. A similar ring assembly of F-BAR proteins is observed along the contractile ring of cell division [33]. For $C_{\text{rod}} < 0$, the rods bend the membrane in the inner direction (opposite to the original membrane curve) such that the rods locally form a saddle shape, in which the two principal curvatures have opposite signs. Thus, the network structures are stabilized by the positive (opposite) side curvature $C_{\text{side}} > 0$ but not

by $C_{\text{side}} < 0$. The inner membrane of mitochondria has a much larger surface area than the outer one and forms numerous invaginations called cristae, which have tubular and planar structures. Previously, we demonstrated that the constraint of the outer membrane can induce such invaginations [34]. The tubular invagination can be also induced by membrane bending of the protein rods. It is likely that the combination of these two mechanisms results in the formation of the cristae in mitochondria.

Here, we employed Langevin dynamics in which hydrodynamic interactions are neglected. Since the static stability of the network branch is the key factor, we do not expect the obtained C_{side} dependence to be qualitatively changed by hydrodynamic interactions. However, the condition for network formation can be modified. The network formation is observed in the phase separation of two fluids of different viscosity [35]. Thus, when the rod-adsorbed regions have higher viscosity, the network formation can be enhanced.

We have revealed that in the addition to the spontaneous curvature C_{rod} along the protein rods, the perpendicular spontaneous curvature C_{side} significantly influences the protrusion of membrane tubules. The percolated-network structure of the rod assembly has a long lifetime for $C_{\text{side}} < 0$ because the saddle membrane shape at branches of the rod network is stabilized by the opposite curvature of C_{side} with respect to C_{rod} . Remarkably, the temporal-network formation suppresses tubulation despite having a minor effect on the equilibrium property.

The numerical calculations were partly carried out on SGI Altix ICE 8400EX at ISSP Supercomputer Center, University of Tokyo. This work was partially supported by a Grant-in-Aid for Scientific Research on Innovative Areas "Fluctuation & Structure" (No. 25103010) from the Ministry of Education, Culture, Sports, Science, and Technology of Japan.

* noguchi@issp.u-tokyo.ac.jp

- [1] J. Zimmerberg and M. M. Kozlov, *Nat. Rev. Mol. Cell Biol.* **7**, 9 (2006).
- [2] T. Baumgart, B. R. Capraro, C. Zhu, and S. L. Das, *Annu. Rev. Phys. Chem.* **62**, 483 (2010).
- [3] L. Johannes, C. Wunder, and P. Bassereau, *Cold Spring Harbor Perspect. Biol.* **6**, a016741 (2014).
- [4] J. Rossy, Y. Ma, and K. Gaus, *Curr. Opin. Chem. Biol.* **20**, 54 (2014).
- [5] T. Itoh and P. De Camilli, *Biochim. Biophys. Acta* **1761**, 897 (2006).
- [6] M. Masuda and N. Mochizuki, *Semin. Cell Dev. Biol.* **21**, 391 (2010).
- [7] C. Mim and V. M. Unger, *Trends Biochem. Sci.* **37**, 526 (2012).
- [8] A. Frost, R. Perera, A. Roux, K. Spasov, O. Destaing, E. H. Egelman, P. De Camilli, and V. M. Unger, *Cell*

- 132**, 807 (2008).
- [9] B. Sorre, A. Callan-Jones, J. Manzi, B. Goud, J. Prost, P. Bassereau, and A. Roux, *Proc. Natl. Acad. Sci. USA* **109**, 173 (2012).
- [10] C. Zhu, S. L. Das, and T. Baumgart, *Biophys. J.* **102**, 1837 (2012).
- [11] Y. Tanaka-Takiguchi, T. Itoh, K. Tsujita, S. Yamada, M. Yanagisawa, K. Fujiwara, A. Yamamoto, M. Ichikawa, and K. Takiguchi, *Langmuir* **29**, 328 (2013).
- [12] R. Lipowsky, *Faraday Discuss.* **161**, 305 (2013).
- [13] P. B. Canham, *J. Theor. Biol.* **26**, 61 (1970).
- [14] W. Helfrich, *Z. Naturforsch* **28c**, 693 (1973).
- [15] J.-B. Fournier, *Phys. Rev. Lett.* **76**, 4436 (1996).
- [16] D. Kabaso, E. Gongadze, P. Elter, U. van Rienen, J. Gimsa, V. Kralj-Iglič, and A. Iglič, *Mini Rev. Med. Chem.* **11**, 272 (2011).
- [17] A. Iglič, H. Hägerstrand, P. Veranič, A. Plemenitaš, and V. Kralj-Iglič, *J. Theor. Biol.* **240**, 368 (2006).
- [18] A. Arkhipov, Y. Yin, and K. Schulten, *Biophys. J.* **95**, 2806 (2008).
- [19] H. Yu and K. Schulten, *PLoS Comput. Biol.* **9**, e1002892 (2013).
- [20] M. Simunovic, A. Srivastava, and G. A. Voth, *Proc. Natl. Acad. Sci. USA* **110**, 20396 (2013).
- [21] N. Ramakrishnan, J. H. Ipsen, and P. B. Sunil Kumar, *Soft Matter* **8**, 3058 (2012).
- [22] N. Ramakrishnan, P. B. Sunil Kumar, and J. H. Ipsen, *Biophys. J.* **104**, 1018 (2013).
- [23] G. S. Ayton, E. Lyman, V. Krishna, R. D. Swenson, C. Mim, V. M. Unger, and G. A. Voth, *Biophys. J.* **97**, 1616 (2009).
- [24] H. Noguchi, *EPL* **108**, 48001 (2014).
- [25] H. Noguchi, *J. Phys. Soc. Jpn.* **78**, 041007 (2009).
- [26] H. Noguchi and G. Gompper, *Phys. Rev. E* **73**, 021903 (2006).
- [27] H. Shiba and H. Noguchi, *Phys. Rev. E* **84**, 031926 (2011).
- [28] H. Noguchi, *EPL* **102**, 68001 (2013).
- [29] See supplemental material at <http://XXX> for details of the simulation method, movies of the tubulation from flat membranes, and sequential snapshots of vesicle deformations.
- [30] H. Noguchi, *J. Chem. Phys.* **134**, 055101 (2011).
- [31] K. Hukushima and K. Nemoto, *J. Phys. Soc. Jpn.* **65**, 1604 (1996).
- [32] Y. Okamoto, *J. Mol. Graph. Model.* **22**, 425 (2004).
- [33] D. Laporte, V. C. Coffman, I.-J. Lee, and J.-Q. Wu, *J. Cell Biol.* **192**, 1005 (2011).
- [34] A. Sakashita, M. Imai, and H. Noguchi, *Phys. Rev. E* **89**, 040701(R) (2014).
- [35] H. Tanaka, *J. Phys. Condens. Matter* **12**, R207 (2000).